



# Immobilization of laccases onto cellulose nanocrystals derived from waste newspaper: relationship between immobilized laccase activity and dialdehyde content

Xinyue Xing · Ying Han · Qiwen Jiang · Yang Sun · Xing Wang · Guiyang Qu · Guangwei Sun · Yao Li

Received: 6 August 2020 / Accepted: 30 March 2021 / Published online: 9 April 2021  
© The Author(s), under exclusive licence to Springer Nature B.V. 2021

**Abstract** The purpose of this work is to evaluate the possibility of using cellulose nanocrystals (CNC) derived from waste newspaper as a carrier for immobilizing laccases. Firstly, the cellulose nanocrystals extracted from waste newspaper were oxidized with sodium periodate, and the hydroxyl groups on the second and third carbons (C2 and C3) of the CNC molecules were converted to dialdehyde groups. Then, the laccase was successfully immobilized on the dialdehyde-modified cellulose nanocrystals (DMC) through covalent bonding. The DMC was characterized using zeta potential, Fourier-transform infrared spectroscopy, X-ray diffraction, scanning electron microscopy, and transmission electron microscopy,

and the relationship between the activity of the immobilized laccase and the dialdehyde group content of the DMC was thoroughly investigated. It was found that the yield of the laccase immobilization is 64.94%, and the highest activity of the immobilized laccase (1.108 U/mg) is obtained at an aldehyde content of the DMC equal to 50.64%, a mass ratio of the carrier to the laccase equal to 45:3, a pH of 4.5, and a reaction time of 2 h. Compared to the free laccase, the immobilized laccase exhibits excellent stability in a wider range of pH values and temperatures. Furthermore, the immobilized laccase showed excellent reusability as evidenced by its retained relative activity of 67% after 6 cycles.

**Supplementary Information** The online version contains supplementary material available at <https://doi.org/10.1007/s10570-021-03867-x>.

X. Xing · Y. Han (✉) · X. Wang (✉) ·  
G. Qu · G. Sun · Y. Li  
Liaoning Key Laboratory of Pulp and Papermaking  
Engineering, Dalian Polytechnic University,  
Dalian 116034, China  
e-mail: hanying@dipu.edu.cn

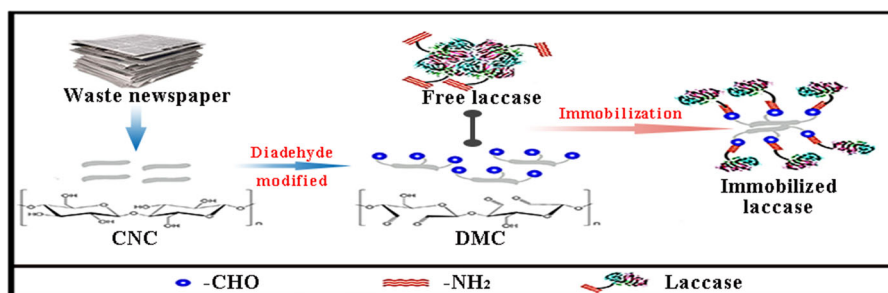
X. Wang  
e-mail: wangxing@dipu.edu.cn

Y. Han · X. Wang  
State Key Laboratory of Pulp and Paper Engineering,  
South China University of Technology,  
Guangzhou 510640, China

Q. Jiang  
Jiangsu Co-Innovation Center of Efficient Processing  
and Utilization of Forest Resources, Nanjing Forestry  
University, Nanjing 210037, China

Y. Sun  
Department of Chemistry, Faculty of Engineering, Gunma  
University, Kiryu, Gunma 376-8515, Japan

## Graphic abstract



**Keywords** Waste newspaper · Cellulose nanocrystals · Laccase · Immobilized enzyme · Biomass

## Introduction

Laccases (benzenediol: oxygen oxidoreductases, EC 1.10.3.2) are a family of multi-copper oxidases with high activity and a remarkable ability to oxidize a variety of multiple substrates, preferably (poly) phenolic compounds. Owing to these remarkable properties, they can be used as potential industrial catalysts and applied to waste water treatment (Daassi et al. 2013; Zeng et al. 2011), delignification of pulp (Fillat et al. 2010), and dye decolorization (Bayramoglu et al. 2010; Thakur and Gupta 2014).

However, free laccases due to drawbacks such as low stability and high recovery costs have limited industrial use, therefore, in order to resolve these limitations, they can be immobilized on an insoluble support (Fernandez-Fernandez et al. 2013). The immobilization of laccases also improves their properties, such as activity and stability under severe conditions. Additionally, immobilized laccases have great advantages over free laccases in terms of reusability. The most important factors affecting the properties of immobilized laccases include the insoluble support and the laccases immobilization technique; pH, the reaction time, and the enzyme dosage also determine the performance of immobilized laccases (Cristóvão et al. 2011).

Several methods, including covalent bonding (Cinotto et al. 2015), encapsulation (Gill et al. 2018),

adsorption (Chen et al. 2015b), and electrospray deposition (Castrovilli et al. 2020) can be employed to immobilize laccases on a support. The characteristics of an ideal support/carrier include a high surface area, biocompatibility, good stability, physical resistance, high binding capacity, and availability at a low cost. Various supports such as surfactant-modified clay material (Chang et al. 2016), sol-gel-derived silica (Qiu and Huang 2009), copper ions-chelated chitosan (Bayramoglu et al. 2012), and ionic liquid-modified cellulose acetate (Mocellini et al. 2011) have been reported specifically for the immobilization of laccases. However, immobilization based on these methods either uses organically synthesized materials, some of which may not be environmentally friendly, or needs complicated operating procedures, which results in a low rate of enzyme immobilization. Native cellulose, a readily available, environmentally friendly, and renewable material, has been used as a support for enzyme immobilization recently. Frazão et al. used bacterial cellulose as a support for commercial laccase immobilization and showed that the thermal stability of the immobilized laccase significantly increased at 60 and 70 °C (Frazão et al. 2014). Zhang et al. immobilized laccase onto chitosan using glutaraldehyde as a crosslinker and used it to removal 2,4-dichlorophenol, the immobilized laccase showed a high enzyme activity and excellent storage stability (Zhang et al. 2009). Cristóvão et al. utilized agricultural residue (green coconut fibers) as a support for commercial laccase immobilization by physical adsorption and reported that the immobilized laccase lost about 30 and 45% of its initial enzyme activity after 5 and 13 oxidation cycles respectively (Cristóvão et al. 2011). Although these studies have developed an

effective support for the laccase immobilization, the macroscale dimensions and less functional groups of native cellulose limit its application in the immobilization of enzymes. On the contrary, cellulose nanocrystals as natural nanomaterials possess unique properties such as nanoscale dimensions, excellent mechanical properties, a high specific surface area, and high strength (Benini et al. 2018; Li et al. 2015). Moreover, cellulose nanocrystals contain plenty of hydroxyl groups in their structure that can be used for surface modification. These properties make it possible for the modified CNC to be utilized for the immobilization of laccases.

Cellulose nanocrystals are usually extracted from ramiess, microcrystalline cellulose, cotton fibers, bacteria, and wood pulps. In spite of the availability of a wide variety of raw materials, it appears that developing techniques for exploiting residual biomass as a CNC source is practically sensible. Moreover, the production of CNC from waste newspaper will provide a new process of paper recycling and possibly solve the problem of the byproducts of paper-to-paper recycling. Therefore, research into the immobilization of laccases onto a support based on cellulose nanocrystals derived from waste newspaper is of vital importance due to its novelty and environmental advantages.

In the present work, we developed a CNC-based support for the immobilization of laccases. First, cellulose nanocrystals were extracted from waste newspaper by sulfuric acid hydrolysis. Then, the laccase was immobilized onto the CNC activated by sodium periodate ( $\text{NaIO}_4$ ), which can selectively oxidize the hydroxyl groups in cellulose nanocrystals to 2,3-dialdehyde functionalities. The aldehyde functional groups can further react with the amine groups of the laccase, which will lead to the immobilization of the laccase molecules. In the current study, the properties of the CNC and the factors influencing the laccase immobilization were investigated, and a range of characteristics such as the optimum catalytic conditions and the reusability of the immobilized laccase were assessed and compared with those of the free laccase.

## Materials and methods

### Materials

The properties of waste newspaper were presented in supplementary Table S1. Sulfuric acid ( $\text{H}_2\text{SO}_4$ ) and Hydroxylamine hydrochloride ( $\text{NH}_2\text{OH}\cdot\text{HCl}$ ) were purchased from Tianjin Kemiou Chemical Reagent Co., Ltd. (Tianjin, China). Sodium Periodate ( $\text{NaIO}_4$ ) and 3-ethyl-benzothiazoline-6-sulphonic acid (ABTS) were purchased from Shanghai Aladdin Biochemical Technology Co., Ltd. (Shanghai, China). Ethylene glycol was purchased from Sinopharm Chemical Reagent Co., Ltd. (Shanghai, China). Laccase was purchased from Novozymes (China) Biopharma Co., Ltd. (Tianjin, China). All chemicals were analytical grade and without further purification.

### Waste newspaper derived cellulose nanocrystals (CNC)

CNC was prepared following a procedure described with Jiang et al. (2020). In a typical experiment, waste newspaper (3 g) was hydrolyzed by sulfuric acid (60 mL, 60%) solution and stirred at 50 °C for 90 min. The resulting suspension was diluted 10 times with deionized water to quench the hydrolysis and thoroughly washed by repeated centrifugation several times. The remaining solid was dialyzed against deionized water to neutral to remove residual acid. Finally, the suspension was sonicated at room temperature for 30 min to obtain a uniform CNC dispersion. The obtained CNC dispersion was then diluted using deionized water to a concentration of 1 wt% and stored at 4 °C for further experiments. Dry cellulose nanocrystals samples are obtained by freeze-drying the suspensions.

### Dialdehyde modified CNC (DMC) production

Theoretically,  $\text{NaIO}_4$  can selectively oxidize cellulose, convert its hydroxyl groups on C2, C3 to aldehyde groups, and form DMC by oxidative cleavage between the C2 and C3 bonds of the glucose unit (Lu et al. 2016). Briefly, CNC (0.5 wt%) was mixed with the required amount of sodium periodate (sodium periodate to CNC weight ratio of 4) and stirred at 45 °C in a light-shielded environment for 2, 3, 4, 5, 6, 7, and 8 h, respectively. Upon completion,

20 mL of ethylene glycol was added to stop the reaction. The mixture was centrifuged, dialyzed and freeze-dried, and then the powdered DMC was obtained. The yield and aldehyde group content of DMC was calculated as shown in supplementary data.

### Immobilization of laccase

In general, the immobilized laccase was prepared by Schiff base reaction between the amino group in the enzyme protein and aldehyde groups of DMC (Chen et al. 2015b). The laccase was prepared according to the complete randomized design to obtain information about the following processing factors: (A) aldehyde group content; (B) carrier dosage; (C) pH; (D) reaction time. Each of these factors was tested at seven variables (view supplementary Table S2).

The freeze-dried DMC sample was placed into a 1000-fold dilution of laccase at a set ratio and reacted at 25 °C and 80 rpm at different reaction time, and then the reaction mixture was placed in a 5 °C refrigerator statically for 14 h to equilibrate the temperature. Upon completion, the DMC gels were filtered out and the surface of the gels were washed three times quickly with phosphate-citrate buffer and collected filtrate to measure the free laccase activities (U/mg). The isolated immobilized enzyme was stored in a refrigerator at 4 °C, and then measured the immobilized enzyme activity (U/mg). The immobilized laccase activity assay was determined by ABTS as a substrate and the detailed method shown in the supplementary data.

### The stability and reusability of immobilized laccase

To evaluate the storage stability, free and immobilized laccase were stored at 4 °C for 24 h in 100 mM citrate buffer (pH 4.5) and 100 mM citrate buffer (pH 3.5), respectively. During the time, samples were taken every 2 h for activity assay. Immediately prior to laccase activity assay, immobilized laccase were washed once with the corresponding buffer solution. Free and immobilized laccase activity was determined over the time under the experimental conditions described in the supplementary data. All the tests were performed in triplicate. The stability was evaluated by relative activity. Relative activity (%) was defined as the ratio of the laccase activity at a certain

time of laccase storage to the initial enzyme activity ( $t = 0$ ) (Frazão et al. 2014).

To study the reusability of immobilized laccase, six consecutive cycles of ABTS oxidation reaction were performed under magnetic stirring at 100 rpm. Each cycle was carried out at 25 °C for 10 min (complete ABTS oxidation). The immobilized laccase activity assay was determined as previously described. At the end of each cycle, the reaction was stopped by substrate removal, and the immobilized laccase was washed three times with 100 mM citrate buffer (pH 3.5). Afterwards, the process was repeated with a fresh substrate. Moreover, repeat tests were performed for each assay. The reusability along the cycles were evaluated by relative activity. Relative activity (%) was defined as the ratio of the laccase activity at the end of each cycle to the enzyme activity at the first cycle, and the original activity of the immobilized laccase was defined as 100%.

### Characterization analysis

The Zeta potential of samples was analyzed by a Zetasizer Nano ZS instrument (Malvern Instruments Ltd., UK). All the sample suspensions (0.05 wt%) were ultrasonically treated for 30 min before analysis. Fourier spectra were measured by a Fourier transform infrared spectrometer (LR-649-12-C, Shanghai Mountain Science Instrument Co., Ltd., China). The CNC and DMC were crushed into powder, thoroughly mixed with KBr and then compressed into slices. The spectra were recorded from 400 to 4000  $\text{cm}^{-1}$  with a resolution of 4  $\text{cm}^{-1}$ . The crystallinity of the cellulose was studied by XRD. XRD spectra was detected at 45 kV and 40 mA from 10° to 50° at a rate of 4°/min with a Ni-filtered Cu K $\alpha$ 1 radiation ( $\lambda = 1.542 \text{ \AA}$ ). The crystallinity was calculated by the empirical method:  $X_c = (I_{200} - I_{am})/I_{200} \times 100\%$ , where  $I_{200}$  is the maximum intensity of the diffraction from the (200) lattice peak ( $2\theta = 22^\circ$ ) and  $I_{am}$  is the diffraction intensity at  $2\theta = 18^\circ$ . The morphology of the CNC and DMC were analyzed by field emission scanning electron microscope (JSM-7800F, JEOL Ltd., Japan). The samples were coated with gold before processed. The TEM image of CNC and DMC were analyzed by a transmission electron microscopy (JEM-2100UHR, JEOL Ltd., Japan) with an accelerating voltage of 120 kV. The suspension was deposited onto a carbon supported copper grid after a 30 min ultrasonic

process and then dyed by dropping Phosphotungstic acid. After holding for 40 s, the excess water was carefully removed by filter paper. The samples were completely air dried prior to imaging.

## Results and discussion

### Effect of oxidation time on properties of DMC

Sodium periodate oxidation is a specific reaction to convert the hydroxyl groups on the second and third carbons (C2 and C3) of cellulose nanocrystals molecules to aldehyde groups without significant side reactions and to form dialdehyde-modified cellulose nanocrystals (Lu et al. 2016) (see supplementary Fig. S1). The influence of reaction time on the aldehyde group content, crystallinity, yield, and zeta potential of the DMC was studied. As presented in Fig. 1, the aldehyde group content of the DMC increases as the duration of oxidation reaction is extended. Nevertheless, the crystallinity of dialdehyde-modified cellulose nanocrystals greatly decreases when the reaction time exceeds 4 h (see supplementary Fig. S2). During this period, part of the crystalline region was destructed, which not only improved the internal accessibility of cellulose, but also may be beneficial to produce more aldehyde group. As presented in Fig. 1, the generation rate of the aldehyde group content decreased slightly after 4 h, which may be ascribed to formation of acetals and

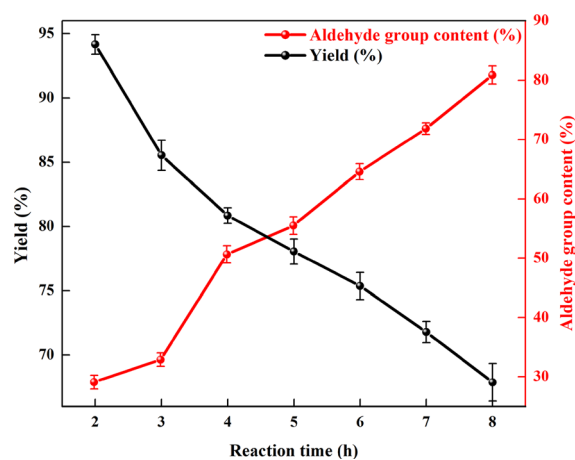


**Fig. 1** Effect of the oxidation time on the aldehyde group content and yield of the DMC; standard deviations of the measurements made in triplicate are shown

hemiacetals by the aldehyde groups react with adjacent hydroxyl groups as the aldehyde groups content increased (Sun et al. 2015). Longer reaction times also reduce the yield of DMC. Based on the procedures published (Calvini et al. 2006), there may be two reactions giving rise to loss of the yield and crystallinity of reaction during the  $\text{NaIO}_4$  oxidation process in this study: a rapid initial phase ( $t^{0.5} = 120$  min) involving oxidation of amorphous regions of CNC, followed by a slower second reaction ( $t^{0.5} = 20$  h) involving the oxidation of crystallite surface of CNC. Furthermore, one of the other reasons for the loss of the yield of reaction during the  $\text{NaIO}_4$  oxidation process could be formation of soluble fragments.

As presented in Fig. 2, the zeta potential falls with increasing the reaction time, which is attributed to the increase in the aldehyde group content of the DMC. The surface of cellulose contains electronegative groups such as hydroxyl and carboxyl groups which are ionized in aqueous solution to make the surface of the cellulose negatively charged. However, the electronegativity of cellulose increased as the of the oxidation time, which is attributed to the oxidation of the hydroxyl groups at the C2 and C3 positions of cellulose molecule to uncharged aldehyde groups. In addition, the further reactions of formed aldehyde groups with neighboring hydroxyl groups to form acetals and hemiacetals, may also be responsible for the lowered electronegativity (Sun et al. 2015).

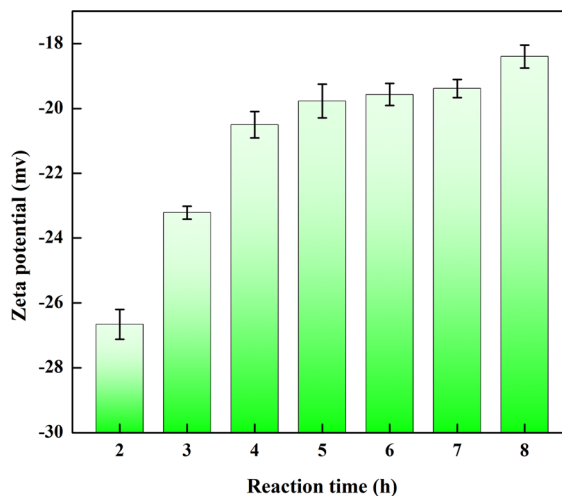


**Fig. 2** Effect of the oxidation time on the zeta potential of the DMC; standard deviations of the measurements made in triplicate are shown

Therefore, from 2 to 8 h of reaction time, the zeta potential of DMC decreases from  $-51.23$  mv (the zeta potential of the CNC) to  $-26.7$  mv or even  $-18.4$  mv.

### Characteristics of CNC and DMC

Figure S3 delineates the Fourier-transform infrared (FTIR) spectra of the CNC and DMC, and supplementary Fig. S4 depicts the FTIR spectra of the DMC at a sodium periodate oxidation time of 2–8 h. Overall, the characteristic peak at  $3335\text{ cm}^{-1}$  is due to the stretching vibration of  $-\text{OH}$  groups (Peng et al. 2009), and the peak at  $1644\text{ cm}^{-1}$  is related to the bending vibration of  $\text{H}_2\text{O}$  (Zaman et al. 2013); also, the significant band at  $2902\text{ cm}^{-1}$  is attributed to the symmetric C–H vibrations (Sun et al. 2015). Compared to the CNC, the peak of carbonyl groups of sample DMC-4 h appears at  $1735\text{ cm}^{-1}$  (Gong et al. 2013). The change in the hemiacetal vibration peak at  $895\text{ cm}^{-1}$  is not obvious because the aldehyde groups in the DMC are present in more than one form (Spedding 1960).

The X-ray diffraction patterns of the CNC and DMC (at a sodium periodate oxidation time of 4 h) are presented in Fig. 3 and supplementary Fig. S5. The CNC and DMC possess the typical diffraction peaks of cellulose I with absorption peaks at  $2\theta$  angles of 14.8, 16.5, and 22.6, which are assigned to the crystalline

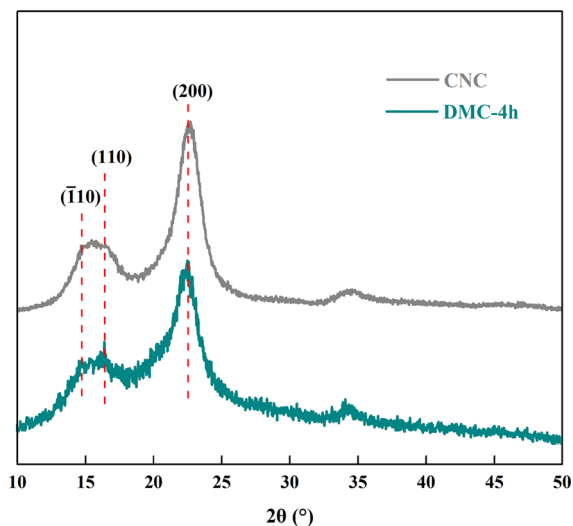


**Fig. 3** X-ray diffraction patterns of the CNC and DMC (at a sodium periodate oxidation time of 4 h)

planes of  $(\bar{1}10)$ ,  $(110)$ , and  $(200)$  respectively (French 2013; Peng et al. 2013). After the oxidation, there was no big change in the absorption peaks angle, thus implying that  $\text{NaIO}_4$  caused little change on the properties of CNC (Sun et al. 2015). However, it is clear that the diffraction peaks of the DMC are significantly reduced, indicating that its crystallinity may be decreased to some degree owing to the oxidation. In fact, the crystallinity of the dialdehyde-modified cellulose nanocrystals is 61.38%, which is slightly lower than that of the cellulose nanocrystals (77.56%). The decreased crystallinity of the DMC may be ascribed to the opening of the glucopyranose rings and to the severe destruction of the regular structure of the CNC (Yang et al. 2013).

The images of the transmission electron microscopy (TEM) and scanning electron microscopy (SEM) of the CNC and DMC are presented in Fig. 4. The results reveal that, compared with the CNC, the DMC still has a rod-like structure with a length of  $95 \pm 20$  nm and a width of  $5 \pm 2.5$  nm; however, the DMC fibers are smaller and thinner than the CNC fibers with a length of 142.87 nm and a width of 9.67 nm. Besides, the DMC fibers are interwoven and form an aerogel-like network after the sample is freeze-dried. As can be seen in Fig. 4a, a large number of pores are formed due to the interweave of the fibers, which increases the specific surface area of the DMC, thereby enhancing the immobilization of the enzymes.

### Optimization of laccase immobilization

The effect of the aldehyde group content of the MDC on laccase immobilization (in terms of the variation in laccase adsorption ratio) is plotted in Fig. 5a. It can be seen that the rate of the laccase immobilization first increases rapidly and then plateaus gradually as the aldehyde group content of the DMC rises. The maximum activity of the immobilized laccase (the maximum activity of the immobilized laccase is defined as 100%) is obtained when the aldehyde group content of the DMC is 50.64%, which corresponds to a rate of laccase adsorption equal to 70.77%. When the aldehyde content of DMC is set at 80.85%, although the maximum immobilization rate of laccase is reached, the relative activity is only 43.32%. This transition may be due to the reasons that at low aldehyde content, the immobilized laccase was not

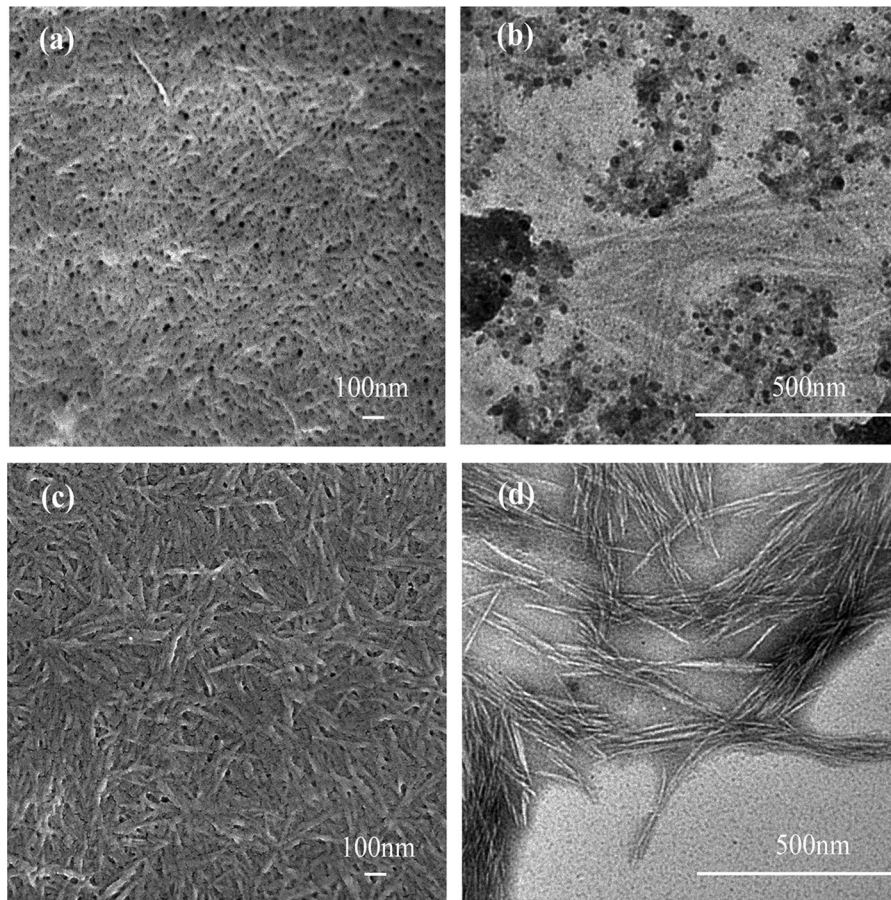


**Fig. 4** SEM images of **a** DMC and **c** CNC and TEM images of **b** DMC and **d** CNC

sufficiently cross-linked and the unbound free laccase was released into the aqueous medium. At high aldehyde content, the laccase is excessively cross-linked, resulting in decreased laccase flexibility and inactivation of laccase (Cao et al. 2016; Qiu et al. 2005).

Figure 5b illustrates the effect of enzyme dosage, which is defined as the mass ratio of the DMC to the laccase, on the rate of the laccase immobilization and the relative activity of the immobilized laccase when the aldehyde group content of the DMC and the oxidation reaction time are set at 50.64% and 4 h respectively. It is obvious that the rate of the laccase immobilization drops gradually as the enzyme dosage exceeds 40:3, that is, the rate of the laccase immobilization decreases as the amount of the laccase rises. When the change in the rate of the laccase immobilization is not noticeable, an increase in the amount of the laccase can effectively improve the relative

activity of the immobilized laccase. The maximum activity of the immobilized laccase is obtained when the carrier dosage is equal to 45:3.

Figure 5c presents the variations in the relative activity and immobilization rate of the laccase in a pH range of 3.0–6.0. It is clear that the maximum rate of the laccase immobilization can be obtained at a pH of 3.5. However, the maximum activity of the immobilized laccase is achieved at a pH of 4.5, implying that the pH of the optimum reaction medium for the immobilized laccase shifts in the acidic direction. When the pH is lower than 4.0, the positively charged laccase reacts with the negatively charged DMC, hence the rate of the laccase immobilization improves. Nonetheless, since the activity of the immobilized laccase is more influenced by the pH of the reaction medium (see supplementary Fig. S6), the optimum pH for the preparation of the immobilized laccase is set at 4.5.

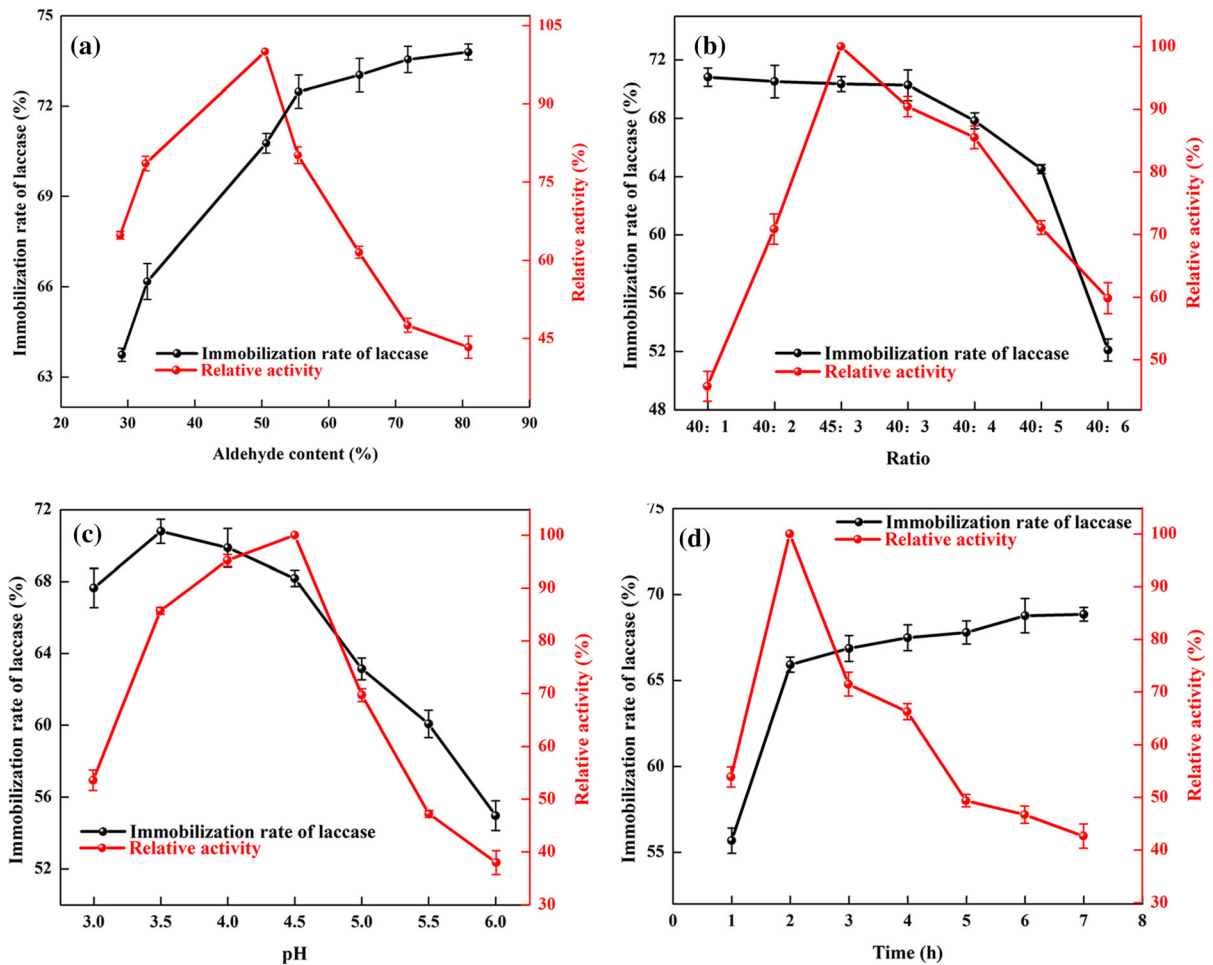


**Fig. 5** Variations in the relative activity and immobilization rate of the laccase with: **a** the aldehyde group content of the DMC (at a mass ratio of the DMC to the laccase of 40:4, a pH of 4.5, and a reaction time of 2 h); **b** enzyme dosage (at an aldehyde group content of the DMC equal to 50.64%, a pH of 4.5, and a reaction time of 2 h); **c** pH (at an aldehyde group

content of the DMC equal to 50.64%, a mass ratio of the DMC to the laccase of 45:3, and a reaction time of 2 h); **d** reaction time (at an aldehyde group content of the DMC equal to 50.64%, a mass ratio of the DMC to the laccase of 45:3, and a pH of 4.5); standard deviations of the measurements made in triplicate are shown

The effect of the reaction time on the laccase immobilization is also studied. As shown in Fig. 5d, the rate of the laccase immobilization first rises and then gradually plateaus as the reaction time increases; the activity of the immobilized laccase also peaks at a reaction time of 2 h. Moreover, at longer reaction times, the active centers of the laccase molecules bind more strongly with the DMC. Nevertheless, a longer oxidation time reduces the activity of the immobilized laccase since it becomes partially inactivated.

#### Biochemical properties of free and immobilized laccase

According to Fig. 6a delineating the influence of temperature on the activity of the immobilized and free laccase, the activity of the free and immobilized laccase first soars to a maximum and then decreases as temperature rises. The maximum activity of the free and immobilized laccase (when the laccase is immobilized by covalent bonding) is achieved at an optimum temperature of 85 and 90 °C respectively. The change in the optimum temperature shows an increase in the thermal stability of the immobilized



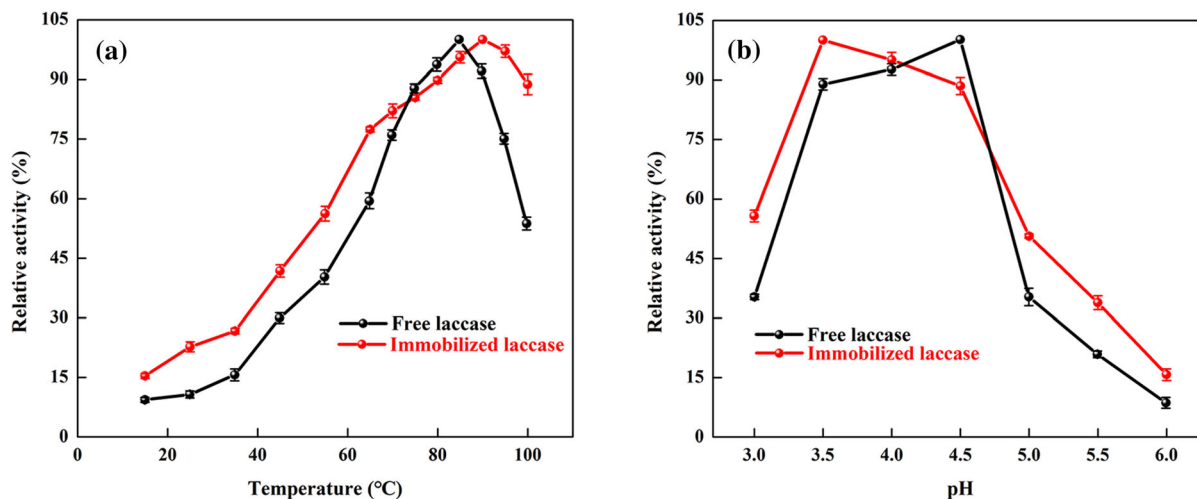


**Fig. 6** Variation in the relative activity of the free and immobilized laccase with: **a** temperature (at a pH of 4.5); **b** pH (at a temperature of 85 °C); the maximal activity is set at

100% using ABTS as a substrate; standard deviations of the measurements made in triplicate are shown

laccase, which was ascribed to the electronegative groups on the carrier and the protons in the solution forming a balanced microenvironment, which was beneficial to enhance the stability of the enzyme (Lee et al. 2012). Furthermore, compared with the free laccase, the relative activity of the immobilized laccase remains at over 80% in a temperature range of 70–100 °C, which proves that the process of immobilization by covalent bonding has enhanced its stability (Qiu et al. 2019).

The impact of the pH of the reaction medium on the activity of the immobilized and free laccase is also investigated in a pH range of 3.0–6.0, as plotted in Fig. 6b. The obtained results indicate that the highest activity of the free laccase in the presence of 2,2'-Azino-bis(3-ethylbenzothiazoline-6-sulfonic acid) diammonium salt (ABTS) as a substrate is obtained at a pH of 4.5. However, after the immobilization of the laccase by covalent bonding, its activity first rises and then declines as pH increases; also, the maximum activity of the immobilized laccase is achieved at a pH of 3.5. This shift in the optimal pH toward strongly acidic values after the immobilization of the laccase may be attributed to the difference in the microstructure of the support and the concentration of hydronium ions in the reaction solution (Chen et al. 2015a; Liu et al. 2020; Ramírez-Montoya et al. 2015).

Secondary structure of free and immobilized laccase

Amide I band ( $1700\text{--}1600\text{ cm}^{-1}$ ) is analyzed by using Fourier self-deconvolution techniques, and the information on the secondary structure of the enzyme protein is obtained (HPIS F, 1999). According to supplementary Fig. S7, the laccase has a dramatic conformational change after immobilization. Previous research shows that the characteristic peaks of  $\beta$ -sheet,  $\alpha$ -helix,  $\beta$ -turn, and random coil region appear in the range of  $1610\text{--}1640\text{ cm}^{-1}$ ,  $1650\text{--}1658\text{ cm}^{-1}$ ,  $1660\text{--}1700\text{ cm}^{-1}$ , and  $1640\text{--}1650\text{ cm}^{-1}$  respectively (Apetri et al. 2006). The band of  $\alpha$ -helix at  $1650\text{ cm}^{-1}$  is intensified after immobilization, while the bands of other structures such as  $\beta$ -sheet and  $\beta$ -turns are weakened.

The percentage of the change in the secondary structure of the laccase during immobilization is estimated by curve-fitting analysis as listed in Table 1. According to the curve-fitting results, the secondary structure of the free laccase is composed of 18.28%  $\alpha$ -helix, 46.44%  $\beta$ -sheet, and 33.81%  $\beta$ -turn. However, the immobilized laccase contains 30.09%  $\alpha$ -helix, 41.58%  $\beta$ -sheet, and 26.5%  $\beta$ -turn. It is obvious that the fraction of  $\alpha$ -helix is increased after the immobilization of the laccase. It is well known that  $\alpha$ -helix structure contains more hydrogen bonds, which gives rise to the rigidity of the laccase molecular structure.

**Table 1** Amide I band deconvolution for the immobilized and free laccase

Sample	Structure		Wavenumber (cm <sup>-1</sup> )	Relative content (%)
Immobilized laccase	$\beta$ -turn	I	1693.14	1.07
	$\beta$ -turn	II	1683.28	5.87
	$\beta$ -turn	III	1668.68	19.56
	$\alpha$ -helix	IV	1651.97	30.09
	$\beta$ -sheet	V	1632.06	33.16
	$\beta$ -sheet	VI	1617.15	8.42
	Other	VII	–	1.83
Free laccase	$\beta$ -turn	I	1693.21	0.54
	$\beta$ -turn	II	1678.24	13.33
	$\beta$ -turn	III	1662.57	19.94
	$\alpha$ -helix	IV	1650.86	18.28
	$\beta$ -sheet	V	1633.48	8.45
	$\beta$ -sheet	VI	1633.17	30.98
	$\beta$ -sheet	VII	1617.04	7.01
Other	VIII	–	1.46	

Conversely, the absence of hydrogen bonds in  $\beta$ -turn structure allows for the higher flexibility of laccase molecules (Sheng et al. 2016). Therefore, as the  $\alpha$ -helix content of the immobilized laccase increases, its  $\beta$ -turn content declines, thus its stability improves.

#### The stability and reusability of immobilized laccase

The storage stability of free and immobilized laccase was evaluated at 4 °C for 24 h at pH 4.5 and pH 3.5, since these are the respective optimal pH values (Fig. 6b). The immobilized laccase were prepared under the conditions of: aldehyde group content of 50.86%; the ratio of carrier to enzyme molecule of 45:3; pH of 4.5 and the immobilization time of 2 h. As can be seen from Fig. 7a, the immobilized laccase retained 96 and 92% of its initial activity after 12 and 24 h of storage, respectively. On the other hand, the free enzyme maintained 57 and 40% of its original activity after 12 and 24 h of storage, respectively. The stability of free laccase showed a decreased trend. This result indicate that stability can be improved by immobilization; and the similar results were also reported by others authors (Cao et al. 2016; Li et al. 2018). The limited freedom of the immobilized laccase, resulted by immobilization, could reduce the

chance of drastic conformational changes and improve the stability of the laccase (Al-Adhami et al. 2002).

One of the advantages of immobilized laccase is reusability, which can also affect cost savings and allow laccase to be used in continuous bioreactor operations (Palanisamy et al. 2017). The reusability of the immobilized laccase is investigated by six consecutive reaction cycles in the presence of ABTS (Fig. 7b). The original activity of the immobilized laccase is defined as 100%. The results indicate that the relative activity of the immobilized laccase declines slowly through the reaction cycles, and the final immobilized laccase still maintains 67% of its original activity after six reaction cycles, which proves the superior reusability of the immobilized laccase (Muhammad Asgher 2012). The reusability of the laccase can effectively reduce costs, which has great significance to the industry. Some researchers have also studied the reusability of other immobilized laccase systems. For instance, Chen et al. investigated the laccase immobilization on bacterial cellulose (BC) membrane by crosslinking-immobilization and retained 69% of the original activity after seven reaction cycles (Chen et al. 2015a). In another work, Ying et al. studied the laccase immobilization on activated poly (vinyl alcohol) by covalent bonding and achieved residual activity of 64% after seven reaction cycles (Shiyu 2002). Compared to these findings, the

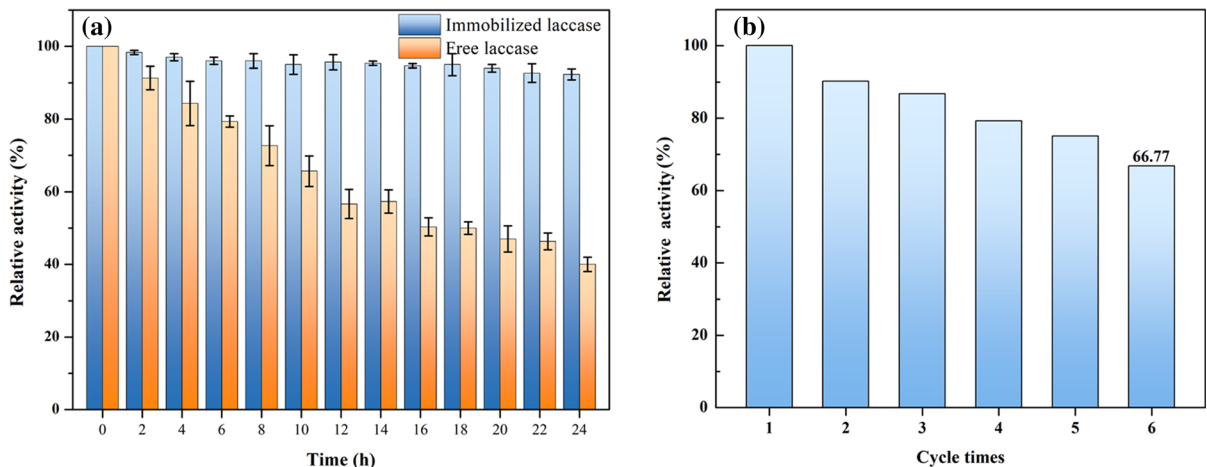


**Fig. 7** The stability of free and immobilized laccase (a); the reusability of the immobilized laccase (b)

laccase immobilized on the dialdehyde-modified cellulose nanocrystals offers ideal reusability.

## Conclusions

In this study, through cross-linking reactions, the laccase is successfully immobilized onto the dialdehyde-modified cellulose nanocrystals produced by oxidizing cellulose nanocrystals in the presence of sodium periodate. The findings demonstrate that, compared to the free laccase, the immobilized laccase exhibits higher activity at the optimal pH of 3.5 and temperature of 85 °C. Moreover, the analysis of the secondary structure of the laccase protein demonstrates that the stability of the laccase is enhanced after immobilization. Furthermore, the immobilized laccase showed excellent reusability as evidenced by its retained relative activity 67% of its original activity after six cycles. Hence, the designed immobilization system provides an effective and simple method for laccase industrial applications.

**Acknowledgments** This research was funded by Liaoning Education Department Project (No. J2020038), Liaoning University Innovation Talent Program in 2020 (No. 20200212), and the Special Financial Grant from the China Postdoctoral Science Foundation (No. 2020T130464).

## Declarations

**Conflict of interest** The authors declare that they have no known competing financial interests or personal relationships

that could have appeared to influence the work reported in this paper.

## References

- Al-Adhami AJH, Bryjak J, Greb-Markiewicz B, Peczyńska-Czoch W (2002) Immobilization of wood-rotting fungi laccases on modified cellulose and acrylic carriers. *Process Biochem* 37:1387–1394. [https://doi.org/10.1016/S0032-9592\(02\)00023-7](https://doi.org/10.1016/S0032-9592(02)00023-7)
- Apetri MM, Maiti NC, Zagorski MG, Carey PR, Anderson VE (2006) Secondary structure of alpha-synuclein oligomers: characterization by raman and atomic force microscopy. *J Mol Biol* 355:63–71. <https://doi.org/10.1016/j.jmb.2005.10.071>
- Bayramoglu G, Yilmaz M, Arica MY (2010) Reversible immobilization of laccase to poly(4-vinylpyridine) grafted and Cu(II) chelated magnetic beads: biodegradation of reactive dyes. *Bioresour Technol* 101:6615–6621. <https://doi.org/10.1016/j.biortech.2010.03.088>
- Bayramoglu G, Gursel I, Yilmaz M, Arica MY (2012) Immobilization of laccase on itaconic acid grafted and Cu(II) ion chelated chitosan membrane for bioremediation of hazardous materials. *J Chem Technol Biotechnol* 87:530–539. <https://doi.org/10.1002/jctb.2743>
- Benini K, Voorwald HJC, Cioffi MOH, Rezende MC, Arantes V (2018) Preparation of nanocellulose from Imperata brasiliensis grass using taguchi method. *Carbohydr Polym* 192:337–346. <https://doi.org/10.1016/j.carbpol.2018.03.055>
- Calvini P, Conio G, Princi E, Vicini S, Pedemonte E (2006) Viscometric determination of dialdehyde content in periodate oxycellulose part II. *Topochem Oxid Cellul* 13:571–579. <https://doi.org/10.1007/s10570-005-9035-y>
- Cao SL et al (2016) Preparation and characterization of immobilized lipase from pseudomonas cepacia onto

- magnetic cellulose nanocrystals. *Sci Rep* 6:20420. <https://doi.org/10.1038/srep20420>
- Castrovilli MC et al (2020) Electrospray deposition as a smart technique for laccase immobilisation on carbon black-nanomodified screen-printed electrodes. *Biosens Bioelectron* 163:112299. <https://doi.org/10.1016/j.bios.2020.112299>
- Chang YT, Lee JF, Liu KH, Liao YF, Yang V (2016) Immobilization of fungal laccase onto a nonionic surfactant-modified clay material: application to PAH degradation. *Environ Sci Pollut Res Int* 23:4024–4035. <https://doi.org/10.1007/s11356-015-4248-6>
- Chen L, Zou M, Hong FF (2015a) Evaluation of fungal laccase immobilized on natural nanostructured bacterial cellulose. *Front Microbiol*. <https://doi.org/10.3389/fmicb.2015.01245>
- Chen X, Li D, Li G, Luo L, Ullah N, Wei Q, Huang F (2015b) Facile fabrication of gold nanoparticle on zein ultrafine fibers and their application for catechol biosensor. *Appl Surf Sci* 328:444–452. <https://doi.org/10.1016/j.apsusc.2014.12.070>
- Cincotto FH, Canevari TC, Machado SAS, Sánchez A, Barrio MAR, Villalonga R, Pingarrón JM (2015) Reduced graphene oxide-Sb<sub>2</sub>O<sub>5</sub> hybrid nanomaterial for the design of a laccase-based amperometric biosensor for estriol. *Electrochim Acta* 174:332–339. <https://doi.org/10.1016/j.electacta.2015.06.013>
- Cristóvão RO, Tavares APM, Brígida AI, Loureiro JM, Boaventura RAR, Macedo EA, Coelho MAZ (2011) Immobilization of commercial laccase onto green coconut fiber by adsorption and its application for reactive textile dyes degradation. *J Mol Catal B Enzym* 72:6–12. <https://doi.org/10.1016/j.molcatb.2011.04.014>
- Daassi D, Zouari-Mechichi H, Prieto A, Martínez MJ, Nasri M, Mechichi T (2013) Purification and biochemical characterization of a new alkali-stable laccase from *Trametes* sp. isolated in Tunisia: role of the enzyme in olive mill waste water treatment. *World J Microbiol Biotechnol* 29:2145–2155. <https://doi.org/10.1007/s11274-013-1380-7>
- Fernandez-Fernandez M, Sanroman MA, Moldes D (2013) Recent developments and applications of immobilized laccase. *Biotechnol Adv* 31:1808–1825. <https://doi.org/10.1016/j.biotechadv.2012.02.013>
- Fillat A, Colom JF, Vidal T (2010) A new approach to the biobleaching of flax pulp with laccase using natural mediators. *Bioresour Technol* 101:4104–4110. <https://doi.org/10.1016/j.biortech.2010.01.057>
- Frazão CJR, Silva NHC, Freire CSR, Silvestre AJD, Xavier AMRB, Tavares APM (2014) Bacterial cellulose as carrier for immobilization of laccase: optimization and characterization. *Eng Life Sci* 14:500–508. <https://doi.org/10.1002/elsc.201400054>
- French AD (2013) Idealized powder diffraction patterns for cellulose polymorphs. *Cellulose* 21:885–896. <https://doi.org/10.1007/s10570-013-0030-4>
- Gill J, Orsat V, Kermasha S (2018) Optimization of encapsulation of a microbial laccase enzymatic extract using selected matrices. *Process Biochem* 65:55–61. <https://doi.org/10.1016/j.procbio.2017.11.011>
- Gong R, Zhang J, Zhu J, Wang J, Lai Q, Jiang B (2013) Loofah sponge activated by periodate oxidation as a carrier for covalent immobilization of lipase. *Korean J Chem Eng* 30:1620–1625. <https://doi.org/10.1007/s11814-013-0102-z>
- Haris PI (1999) FTIR spectroscopic characterization of protein structure in aqueous and non-aqueous media. *J Mol Catal B Enzym* 7:207–221. [https://doi.org/10.1016/S1381-1177\(99\)00030-2](https://doi.org/10.1016/S1381-1177(99)00030-2)
- Jiang Q, Xing X, Jing Y, Han Y (2020) Preparation of cellulose nanocrystals based on waste paper via different systems. *Int J Biol Macromol* 149:1318–1322. <https://doi.org/10.1016/j.ijbiomac.2020.02.110>
- Lee KM, Kalyani D, Tiwari MK, Kim TS, Dhiman SS, Lee JK, Kim IW (2012) Enhanced enzymatic hydrolysis of rice straw by removal of phenolic compounds using a novel laccase from yeast *Yarrowia lipolytica*. *Bioresour Technol* 123:636–645. <https://doi.org/10.1016/j.biortech.2012.07.066>
- Li B et al (2015) Cellulose nanocrystals prepared via formic acid hydrolysis followed by TEMPO-mediated oxidation. *Carbohydr Polym* 133:605–612. <https://doi.org/10.1016/j.carbpol.2015.07.033>
- Li N, Xia Q, Niu M, Ping Q, Xiao H (2018) Immobilizing laccase on different species wood biochar to remove the chlorinated biphenyl in wastewater. *Sci Rep* 8:13947. <https://doi.org/10.1038/s41598-018-32013-0>
- Liu J, Shen X, Zheng Z, Li M, Zhu X, Cao H, Cui C (2020) Immobilization of laccase by 3D bioprinting and its application in the biodegradation of phenolic compounds. *Int J Biol Macromol*. <https://doi.org/10.1016/j.ijbiomac.2020.07.144>
- Lu FF, Yu HY, Zhou Y, Yao JM (2016) Spherical and rod-like dialdehyde cellulose nanocrystals by sodium periodate oxidation: optimization with double response surface model and templates for silver nanoparticles. *Expr Polym Lett* 10:965–976. <https://doi.org/10.3144/expresspolymlett.2016.90>
- Mocellini SK, Franzoi AC, Vieira IC, Dupont J, Scheeren CW (2011) A novel support for laccase immobilization: cellulose acetate modified with ionic liquid and application in biosensor for methyl dopa detection. *Biosens Bioelectron* 26:3549–3554. <https://doi.org/10.1016/j.bios.2011.01.043>
- Muhammed Asgher S (2012) Improvement of catalytic efficiency, thermo-stability and dye decolorization capability of pleurotus ostreatus IBL-02 laccase by hydrophobic sol gel entrapment. *Chem Cent J* 6:110–120. <https://doi.org/10.1186/1752-153X-6-110>
- Palanisamy S et al (2017) A novel laccase biosensor based on laccase immobilized graphene-cellulose microfiber composite modified screen-printed carbon electrode for sensitive determination of catechol. *Sci Rep* 7:41214. <https://doi.org/10.1038/srep41214>
- Peng F, Ren JL, Xu F, Bian J, Peng P, Sun RC (2009) Comparative study of hemicelluloses obtained by graded ethanol precipitation from sugarcane bagasse. *J Agric Food Chem* 57:6305–6317. <https://doi.org/10.1021/jf900986b>
- Peng Y, Gardner DJ, Han Y, Kiziltas A, Cai Z, Tshabalala MA (2013) Influence of drying method on the material properties of nanocellulose I: thermostability and crystallinity.

- Cellulose 20:2379–2392. <https://doi.org/10.1007/s10570-013-0019-z>
- Qiu L, Huang Z (2009) The treatment of chlorophenols with laccase immobilized on sol–gel-derived silica. *World J Microbiol Biotechnol* 26:775–781. <https://doi.org/10.1007/s11274-009-0233-x>
- Qiu G-M, Zhu B-K, Xu Y-Y (2005)  $\alpha$ -Amylase immobilized by Fe<sub>3</sub>O<sub>4</sub>/poly(styrene-co-maleic anhydride) magnetic composite microspheres: preparation and characterization. *J Appl Polym Sci* 95:328–335. <https://doi.org/10.1002/app.21239>
- Qiu X, Qin J, Xu M, Kang L, Hu Y (2019) Organic-inorganic nanocomposites fabricated via functional ionic liquid as the bridging agent for Laccase immobilization and its application in 2,4-dichlorophenol removal. *Coll Surf B Biointerf* 179:260–269. <https://doi.org/10.1016/j.colsurfb.2019.04.002>
- Ramírez-Montoya LA, Hernández-Montoya V, Montes-Morán MA, Jáuregui-Rincón J, Cervantes FJ (2015) Decolorization of dyes with different molecular properties using free and immobilized laccases from *Trametes versicolor*. *J Mol Liq* 212:30–37. <https://doi.org/10.1016/j.molliq.2015.08.040>
- Sheng L, Wang J, Huang M, Xu Q, Ma M (2016) The changes of secondary structures and properties of lysozyme along with the egg storage. *Int J Biol Macromol* 92:600–606. <https://doi.org/10.1016/j.ijbiomac.2016.07.068>
- Shiyu DYWQF (2002) Laccase stabilization by covalent binding immobilization on activated polyvinyl alcohol carrier. *Lett Appl Microbiol* 35:451–456. <https://doi.org/10.1046/j.1472-765X.2002.01196.x>
- Spedding H (1960) Infrared spectra of periodate-oxidised cellulose. *J Chem Soc (Resumed)*. <https://doi.org/10.1039/JR9600003147>
- Sun B, Hou Q, Liu Z, Ni Y (2015) Sodium periodate oxidation of cellulose nanocrystal and its application as a paper wet strength additive. *Cellulose* 22:1135–1146. <https://doi.org/10.1007/s10570-015-0575-5>
- Thakur S, Gupte A (2014) Optimization and hyper production of laccase from novel agaricomycete *Pseudolagarobasidium acaciicola* AGST3 and its application in in vitro decolorization of dyes. *Ann Microbiol* 65:185–196. <https://doi.org/10.1007/s13213-014-0849-4>
- Yang H, Alam MN, van de Ven TGM (2013) Highly charged nanocrystalline cellulose and dicarboxylated cellulose from periodate and chlorite oxidized cellulose fibers. *Cellulose* 20:1865–1875. <https://doi.org/10.1007/s10570-013-9966-7>
- Zaman M, Liu H, Xiao H, Chibante F, Ni Y (2013) Hydrophilic modification of polyester fabric by applying nanocrystalline cellulose containing surface finish. *Carbohydr Polym* 91:560–567. <https://doi.org/10.1016/j.carbpol.2012.08.070>
- Zeng J, Lin X, Zhang J, Li X, Wong MH (2011) Oxidation of polycyclic aromatic hydrocarbons by the bacterial laccase CueO from *E. coli*. *Appl Microbiol Biotechnol* 89:1841–1849. <https://doi.org/10.1007/s00253-010-3009-1>
- Zhang J, Xu Z, Chen H, Zong Y (2009) Removal of 2,4-dichlorophenol by chitosan-immobilized laccase from *Coriolus versicolor*. *Biochem Eng J* 45:54–59. <https://doi.org/10.1016/j.bej.2009.02.005>

**Publisher's Note** Springer Nature remains neutral with regard to jurisdictional claims in published maps and institutional affiliations.